Following the Evolution of Hard Sphere Glasses in Infinite Dimensions under External Perturbations: Compression and Shear Strain

Corrado Rainone,[1,2] Pierfrancesco Urbani,[3] Hajime Yoshino,[4,5] and Francesco Zamponi[1]
[1]LPT, Ecole Normale Supérieure, CNRS UMR 8549, 24 Rue Lhomond, 75005 Paris, France
[2]Dipartimento di Fisica, Sapienza Università di Roma, P.le A. Moro 2, I-00185 Roma, Italy
[3]IPhT, CEA/DSM-CNRS/URA 2306, CEA Saclay, F-91191 Gif-sur-Yvette Cedex, France
[4]Cybermedia Center, Osaka University, Toyonaka, Osaka 560-0043, Japan
[5]Graduate School of Science, Osaka University, Toyonaka, Osaka 560-0043, Japan
(Received 19 July 2014; published 6 January 2015)

We consider the adiabatic evolution of glassy states under external perturbations. The formalism we use is very general. Here we use it for infinite-dimensional hard spheres where an exact analysis is possible. We consider perturbations of the boundary, i.e., compression or (volume preserving) shear strain, and we compute the response of glassy states to such perturbations: pressure and shear stress. We find that both quantities overshoot before the glass state becomes unstable at a spinodal point where it melts into a liquid (or yields). We also estimate the yield stress of the glass. Finally, we study the stability of the glass basins towards breaking into sub-basins, corresponding to a Gardner transition. We find that close to the dynamical transition, glasses undergo a Gardner transition after an infinitesimal perturbation.

DOI: 10.1103/PhysRevLett.114.015701 PACS numbers: 64.70.Q-, 65.60.+a, 83.80.Ab

Introduction.—Glasses are long-lived metastable states of matter, in which particles are confined around an amorphous structure [1,2]. For a given sample of a material, the glass state is not unique: depending on the preparation protocol, the material can be trapped in different glasses, each displaying different thermodynamic properties. For example, the specific volume of a glass prepared by cooling a liquid depends strongly on the cooling rate [1,2]. Other procedures, such as vapor deposition, produce very stable glasses, with higher density than those obtained by simple cooling [3,4]. When heated up, glasses show hysteresis: their energy (specific volume) remains below the liquid one, until a "spinodal" point is reached, at which they melt into the liquid (see, e.g., [2], Fig. 1 and [4], Fig. 2).

The behavior of glasses under shear strain also shows similarly complex phenomena. Suppose to prepare a glass by cooling a liquid at a given rate until some low temperature T is reached. After cooling, a strain γ is applied and the stress σ is recorded. At small γ, an elastic (linear) regime where $\sigma \sim \mu\gamma$ is found. At larger γ, the stress reaches a maximum and then decreases until an instability is reached, where the glass yields and starts to flow (see, e.g., [5], Fig. 3(c) and [6], Fig. 2). The amplitude of the shear modulus μ and of the stress overshoot increase when the cooling rate is decreased, and more stable glasses are reached.

Computing these observables theoretically is a difficult challenge, because glassy states are always prepared through nonequilibrium dynamical protocols. First-principles dynamical theories such as mode-coupling theory [7] are successful in describing properties of supercooled liquids close to the glass state (including the stress overshoot [8]), but they fail to describe glasses at low temperatures and high pressures [9]. The dynamical facilitation picture can successfully describe calorimetric properties of glasses [10], but for the moment it does not allow one to perform first-principles calculations starting from the microscopic interaction potential. To bypass the difficulty of describing all the dynamical details of glass formation, one can exploit a standard idea in statistical mechanics, namely, that metastable states are described by a *restricted* equilibrium thermodynamics for times much shorter than their lifetimes [11,12]. Within schematic models of glasses, this construction was proposed by several authors [13–16] and was formalized through the Franz-Parisi free energy [16] and the "state following" formalism [17–19].

In this Letter we apply the state following construction [16–19] to a realistic model of glass former, made by identical particles interacting in the continuum. For simplicity, we choose here hard spheres in spatial dimension $d \to \infty$, where the method is exact because metastable states have infinite lifetime [13,20,21]. We show that all the properties of glasses mentioned above are predicted by this framework, including the cooling rate dependence of the specific volume (or the pressure) [1,2], the hysteresis observed upon heating glasses [2–4], the behavior of the shear modulus, and the stress overshoot [5,6]. Following [20,22], our method can be generalized (under standard liquid theory approximations) to experimentally relevant systems in $d = 2, 3$ with different interaction potentials, to obtain precise quantitative predictions, as we discuss in the conclusions.

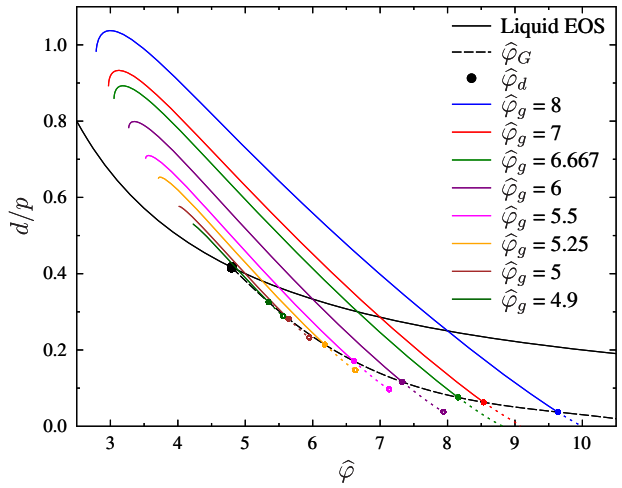

FIG. 1 (color online). Following glasses in (de)compression. Inverse reduced pressure d/p is plotted versus packing fraction $\hat{\varphi} = 2^d\varphi/d$. Both quantities are scaled to have a finite limit for $d \to \infty$. The liquid EOS is $d/p = 2/\hat{\varphi}$. The dynamical transition $\hat{\varphi}_d$ is marked by a black dot. For $\hat{\varphi}_g > \hat{\varphi}_d$, the liquid is a collection of glasses. The glassy EOS are reported as full colored lines that intersect the liquid EOS at $\hat{\varphi}_g$. Upon compression, a glass prepared at $\hat{\varphi}_g$ undergoes a Gardner transition at $\hat{\varphi}_G(\hat{\varphi}_g)$ (full symbols and long-dashed black line). Beyond $\hat{\varphi}_G$ our computation is not correct: glass EOS are reported as dashed lines. For low $\hat{\varphi}_g$ they end at an unphysical spinodal point (open symbol). Upon decompression, the glass pressure falls below the liquid one, until it reaches a minimum, and then grows again until a physical spinodal point at which the glass melts into the liquid.

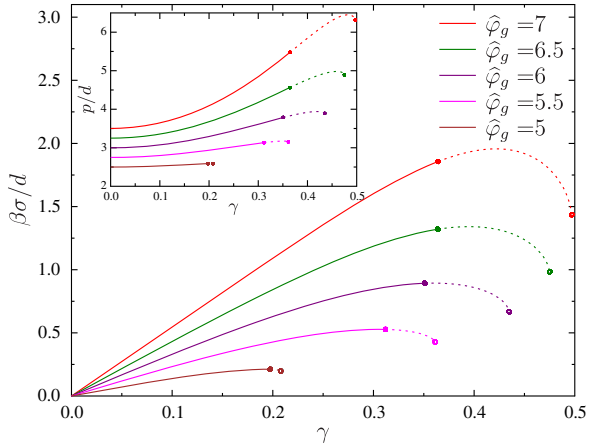

FIG. 2 (color online). Following glassy states prepared at $\hat{\varphi}_g$ upon applying a shear-strain γ. Shear-stress σ (main panel) and reduced pressure p (inset) as a function of strain for different $\hat{\varphi}_g$. Same styles as Fig. 1. Upon increasing shear strain, the states undergo a Gardner transition at $\gamma_G(\hat{\varphi}_g)$. For $\gamma > \gamma_G$ our RS computation is unstable but it predicts a stress overshoot followed by a spinodal point.

The state following construction.—The state following formalism is designed to describe glass formation during slow cooling of a liquid [19]. We present here a short account of this construction; for a more detailed discussion see [16–19] and [23].

Approaching the glass transition, the equilibrium dynamics of the liquid happens on two well-separated time scales [1,2]. On a T-independent fast scale $\tau_{\rm vib}$ particles essentially vibrate in the cages formed by their neighbors. On the slow α-relaxation scale $\tau_\alpha(T)$, which increases fast approaching the glass transition, cooperative processes change the structure of the material. When $\tau_\alpha(T) \gg \tau_{\rm vib}$, the system vibrates for a long time around a locally stable configuration of the particles (a glass), and then on a time scale $\tau_\alpha(T)$ transforms in another equivalent glass. Hence, $\tau_\alpha(T)$ is the lifetime of metastable glasses. The liquid reaches equilibrium if enough different glass states are visited; hence, the experimental time scale (e.g., the cooling rate) should be $\tau_{\rm exp} \gg \tau_\alpha(T)$. For given $\tau_{\rm exp}$, the glass transition temperature T_g is therefore defined by $\tau_{\rm exp} = \tau_\alpha(T_g)$ [1,2]. For $T < T_g$ the system is confined into a given glass with lifetime $\tau_\alpha(T) \gg \tau_{\rm exp}$, which can thus be considered an infinitely long-lived metastable state. Although the system is strictly speaking out of equilibrium in this regime, the slow relaxation is effectively frozen and the material is confined in a thermodynamic equilibrium state *restricted* to a given glass. In fact, if cooling stops at some $T < T_g$, thermodynamic quantities quickly reach time-independent values, that satisfy equilibrium thermodynamic relations. Still, the "thermodynamic" state depends on preparation history, and most crucially on the temperature T_g at which the liquid fell out of equilibrium. Note that aging effects can be neglected here because they happen, for $T < T_g$, on time scales $\tau_{\rm aging} \gg \tau_\alpha(T_g) \sim \tau_{\rm exp}$.

This identification between out of equilibrium states and long-lived metastable states, i.e., between dynamics and thermodynamics, is the core of the state following construction, and allows one to describe the thermodynamic properties of glasses prepared by slow cooling through a thermodynamics formalism [16–19]. Let us now briefly review this formalism. Consider N interacting classical particles, described by coordinates $X = \{x_i\}_{i=1,\ldots,N}$ and potential energy $V(X)$. During a cooling process with time scale $\tau_{\rm exp}$, the system remains equilibrated provided $T \geq T_g$. Define $R = \{r_i\}$ the last configuration visited by the material before falling out of equilibrium; its probability distribution is the equilibrium one at T_g, $P(R) = \exp[-V(R)/T_g]/Z(T_g)$ (here $k_B = 1$). For $T < T_g$, the lifetime of glasses becomes effectively infinite [36]: the material visits configurations X confined in the glass selected by R. This constraint is implemented [16,17] by imposing that the mean square displacement between X and R, $\Delta(X,R) = (d/N)\sum_{i=1}^N (x_i - r_i)^2$, be smaller than a prescribed value Δ^r. The evolution of this glass is followed by changing its temperature T or applying some perturbation γ that changes the potential to V_γ. The free energy of the glass selected by R is, therefore,

$$F_g[T,\gamma;R] = -T\log\int dX e^{-V_\gamma[X]/T}\theta[\Delta^{\mathrm{r}} - \Delta(X,R)].$$

$\theta(x)$ is the Heaviside function. Computing $F_g[T,\gamma;R]$ is a formidably difficult task, because the constraint $\Delta(X,R) \leq \Delta^r$ explicitly breaks translational invariance and prevents one from using standard statistical mechanics methods. One can simplify the problem by computing the average free energy of all glasses that are sampled by liquid configurations at T_g, under the assumption that these glasses have similar thermodynamic properties. We obtain

$$F_g[T,\gamma;T_g] = \overline{F_g[T,\gamma;R]} = \int dR \frac{e^{-V(R)/T_g}}{Z(T_g)} F_g[T,\gamma;R].$$

Note that T_g, which is dynamically selected out of equilibrium, becomes a free parameter in the state following construction. This average can be computed using the replica trick [16], and here we use the simplest replica symmetric (RS) scheme [16–18]. The parameter Δ^r is determined by minimizing the free energy, which is given in [23], Sec. I D.

This state following construction was previously applied to spin glasses in [16–19,37] and describes perfectly the properties of glasses obtained by slow cooling [19]. However, no attempt to apply it to realistic models of glass-forming materials has been previously reported. Here, we achieve this goal by applying the method to a hard sphere system for $d \to \infty$. Technically, the computation uses the methods of [21] in the more complicated state following setting. Because the details are not particularly instructive, we report them in Supplemental Material [23], and in the following we describe our main physical results.

Results: Compression.—As a first application of the method, we consider preparing glasses by slow compression, which is equivalent, for hard spheres, to slow cooling [20]. Note that for hard spheres temperature can be eliminated by appropriately rescaling physical quantities. The system is prepared at low density ρ, particle volume V_s is slowly increased (equivalently, container volume is decreased), and pressure P is monitored. In Fig. 1 we plot the reduced pressure $p = \beta P/\rho$, with $\beta = 1/T$, versus the packing fraction $\varphi = \rho V_s$. At equilibrium, the system follows the liquid equation of state (EOS). Above the so-called *dynamical transition* (or mode-coupling theory transition) density φ_d, glasses appear, and each equilibrium liquid configuration at $\varphi_g > \varphi_d$ selects a glass. As discussed above, φ_g is therefore a free parameter of the state following construction, which can be used to select different glasses corresponding to different preparation protocols. In Fig. 1 we report the EOS of several glasses corresponding to different choices of φ_g. The slope of the glass EOS at φ_g is different from that of the liquid EOS, indicating that when the system falls out of equilibrium at φ_g, the compressibility has a jump, as observed experimentally [20,38]. Following glasses in compression, pressure increases faster than in the liquid (compressibility is smaller) and diverges at a finite *jamming* density $\varphi_j(\varphi_g)$ [20]. However, before jamming is reached, the glass undergoes a *Gardner* transition [21,39], at which individual glass basins become unstable. Because this transition was discussed before [17,18,21,39], we do not insist on its characterization, but note that we can compute precisely the Gardner transition point $\varphi_G(\varphi_g)$ for all φ_g (see [23] for details). Interestingly, as observed in [17,37], the Gardner transition line ends at φ_d, i.e., $\varphi_G(\varphi_g = \varphi_d) = \varphi_d$. This implies that the first glasses appearing at φ_d are marginally stable towards breaking into sub-basins, while glasses appearing at $\varphi_g > \varphi_d$ remain stable for a finite interval of pressures before breaking into sub-basins. Yet, all glasses undergo the Gardner transition at finite pressure before jamming occurs [21].

For a glass selected at φ_g, when the density is higher than φ_G, the simplest RS scheme we used is unstable, and one should perform a more sophisticated computation [17,18,21]. However, we observe that for large enough φ_g the Gardner transition happens at very high pressure and in that case our calculation is a good approximation to the glass EOS at all pressures. For small φ_g instead, the RS calculation gives a wrong prediction, namely, the existence of an unphysical spinodal point at which the glass disappears. We expect, based on the analogy with the results of [18], that a correct calculation will fix this problem.

A given glass prepared at φ_g can be also followed in *decompression*, by decompressing at a relatively fast rate τ_{dec} such that $\tau_{\mathrm{vib}} \ll \tau_{\mathrm{dec}} \ll \tau_{\mathrm{exp}}$. In this case we observe hysteresis (Fig. 1), consistently with experimental results [2–4]. In fact, the glass pressure becomes *lower* than the liquid one, until upon decreasing density a spinodal point is reached, at which the glass becomes unstable and melts into the liquid [40]. Note that pressure "undershoots" (it has a local minimum; see Fig. 1) before the spinodal is reached [40].

Results: Shear.—We investigate now the response of glasses to a shear-strain perturbation. We consider a system compressed in equilibrium up to a density $\hat{\varphi}_g$, where it remains stuck into a glass. Now, instead of compressing the system, we apply a shear-strain γ. In Fig. 2 we report the behavior of shear-stress σ and pressure p versus γ. At small γ we observe a *linear response* elastic regime, where σ increases linearly with γ, $\sigma \sim \mu\gamma$ and pressure increases quadratically above the equilibrium liquid value, $p(\gamma) \sim p(\gamma = 0) + (\beta R/\rho)\gamma^2$. Both the shear modulus μ and the dilatancy $R > 0$ increase with $\hat{\varphi}_g$, indicating that glasses prepared by slower annealing are more rigid.

Upon further increasing γ, glasses enter a nonlinear regime, and undergo a Gardner transition at $\gamma_G(\varphi_g)$ (Fig. 2). Like in compression, we find $\gamma_G(\varphi_d) = 0$, and γ_G increases rapidly with φ_g. For $\gamma > \gamma_G(\varphi_{\mathrm{d}})$, the glass breaks into sub-basins and a full replica symmetry breaking (fRSB)

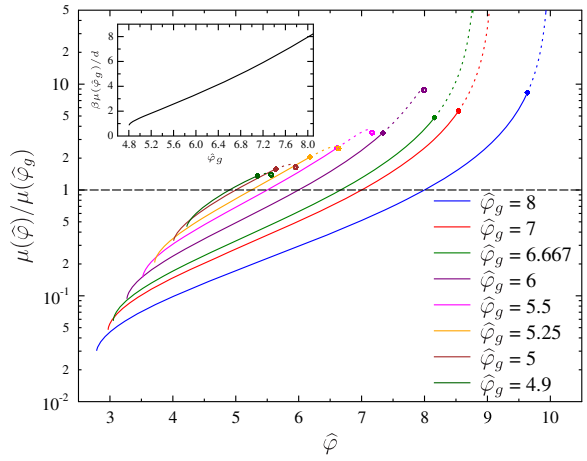

FIG. 3 (color online). Shear modulus versus density for different glasses. Same styles as Fig. 1. In the inset we report $\mu(\hat{\varphi}_g)$ versus $\hat{\varphi}_g$. Note that the dilatancy $R/\rho = (1/2)\hat{\varphi}\partial\mu/\partial\hat{\varphi}$ diverges both at jamming and at the low density spinodal point where the glass melts (see [23]).

calculation is needed. Note that the RS computation predicts a stress overshoot, followed by a spinodal point where the glass basin disappears. We expect that the fRSB computation gives similar results. The spinodal point corresponds to the point where the glass yields and starts to flow. The values of yield strain γ_Y and of yield stress σ_Y are also found to increase with φ_g. These results are qualitatively consistent with the experimental and numerical observations of [5,6].

Results: Compression followed by shear.—One could also consider the case where (i) a liquid is slowly compressed up to φ_g where it forms a glass, (ii) the glass is compressed up to a certain pressure p (Fig. 1), and then (iii) a shear-strain γ is applied. The response to shear strain of these glasses compressed out of equilibrium is qualitatively similar to the one reported in Fig. 2, and we do not report the corresponding curves. Instead, we report in Fig. 3 the behavior of shear modulus μ as a function of density φ for different glasses prepared at different φ_g. For each glass, we find that under compression μ increases with density, and diverges at the jamming point where $p \to \infty$. Note that, as discussed above and in [21], describing the behavior around the jamming density requires a fRSB computation, that we did not perform here.

A useful thermodynamic identity gives the dilatancy $R/\rho = (1/2)\varphi\partial\mu/\partial\varphi$ [41] (see [23]). This implies that the singular behavior of the shear modulus around jamming, which itself is well captured by a fRSB computation [42], should be directly reflected to the dilatancy, as pointed out in [41]. Further work is needed to understand experimental and numerical results [43–45].

Conclusions.—We have applied the state following procedure, developed in the context of spin glasses [16–19], to a microscopic model of a glass former, namely, hard spheres. We considered for simplicity the limit $d \to \infty$, where the method we used is exact, but the calculations can be generalized to obtain *approximated* quantitative predictions in finite d. According to [20,46], the simplest approximation is to use the results reported in this Letter, replacing $\hat{\varphi} = 2^d\varphi/[dy_{\rm HS}^{\rm liq}(\varphi)]$, $y_{\rm HS}^{\rm liq}(\varphi)$ being the contact value of the pair correlation function in the liquid phase, which can be obtained from a generalized Carnahan-Starling liquid EOS [38]. This approximation is expected to be good at large φ_g, but gives poor results for $\varphi_g \sim \varphi_{\rm d}$. Systematic improvements over this approximation can be obtained following the ideas of [20]. It is clear, anyway, that the qualitative shape of the curves we obtained in $d \to \infty$ will not change in finite d, which is also supported by the numerical simulations of [38].

We did not attempt here a more precise quantitative comparison with experimental and numerical data, which we leave for future work, but we showed that the state following method is able to give predictions for many physical observables of experimental interest, and reproduces a quite large number of observations. These include the following. (i) The pressure as a function of density for different glasses (Fig. 1), which displays a jump in compressibility at φ_g [20,38], (ii) the presences of hysteresis and of a spinodal point in decompression in the pressure-density curves (Fig. 1), where we show that more stable glasses (those with higher φ_g) display a larger hysteresis, consistently with the experimental observation of [2–4], the behavior of pressure and shear stress under a shear-strain perturbation (Fig. 2), where we show that (iii) the shear modulus and the dilatancy increase for more stable glasses (higher φ_g). (iv) The shear stress overshoots before a spinodal (yielding) point is reached where the glass yields and starts to flow (Fig. 2) [5,6]. Note, however, that the spinodal (yield) point falls beyond the Gardner transition and therefore its estimate, reported in Fig. 2, is only approximate, a correct computation requires fRSB [21]. Furthermore, (v) we predict that glasses undergo a Gardner transition both in compression (Fig. 1) and in shear (Fig. 2), and we locate the Gardner transition point (see [23]). Finally, we (vi) compute the dilatancy and the shear modulus everywhere in the glass phase (Fig. 3 and [23]) and their behavior close to the jamming transition (see [23]).

This approach thus provides a coherent picture of the phase diagram of glasses in different regimes, under compression and under shear strain, at moderate densities close to the dynamical glass transition and at high densities (pressures) close to jamming. Future work should be directed towards performing systematic comparisons between theory and experiment, and improving the theory, first by performing the fRSB computation, and second by improving the approximation in finite dimensions.

We thank G. Biroli, P. Charbonneau, O. Dauchot, S. Franz, Y. Jin, F. Krzakala, J. Kurchan, M. Mariani, G. Parisi, F. Ricci-Tersenghi, and L. Zdeborová, for

many useful discussions. This work was supported by KAKENHI (No. 25103005 "Fluctuation & Structure" and No. 50335337) from MEXT, Japan, by JPS Core-to-Core Program "Non-equilibrium dynamics of soft matter and informations," and by the European Research Council through ERC Grants Agreement No. 247328 and NPRGGLASS.

[1] A. Cavagna, Phys. Rep. **476**, 51 (2009).
[2] J. C. Dyre, Rev. Mod. Phys. **78**, 953 (2006).
[3] S. F. Swallen, K. L. Kearns, M. K. Mapes, Y. S. Kim, R. J. McMahon, M. D. Ediger, T. Wu, L. Yu, and S. Satija, Science **315**, 353 (2007).
[4] S. Singh, M. Ediger, and J. J. de Pablo, Nat. Mater. **12**, 139 (2013).
[5] D. Rodney, A. Tanguy, and D. Vandembroucq, Model. Simul. Mater. Sci. Eng. **19**, 083001 (2011).
[6] N. Koumakis, M. Laurati, S. U. Egelhaaf, J. F. Brady, and G. Petekidis, Phys. Rev. Lett. **108**, 098303 (2012).
[7] W. Götze, *Complex Dynamics of Glass-Forming Liquids: A Mode-Coupling Theory*, Vol. 143 (OUP, USA, 2009).
[8] J. M. Brader, T. Voigtmann, M. Fuchs, R. G. Larson, and M. E. Cates, Proc. Natl. Acad. Sci. U.S.A. **106**, 15186 (2009).
[9] A. Ikeda and L. Berthier, Phys. Rev. E **88**, 052305 (2013).
[10] A. S. Keys, J. P. Garrahan, and D. Chandler, Proc. Natl. Acad. Sci. U.S.A. **110**, 4482 (2013).
[11] O. Penrose and J. L. Lebowitz, J. Stat. Phys. **3**, 211 (1971).
[12] J. S. Langer, Physica (Amsterdam) **73**, 61 (1974).
[13] T. R. Kirkpatrick and P. G. Wolynes, Phys. Rev. A **35**, 3072 (1987).
[14] T. R. Kirkpatrick and D. Thirumalai, J. Phys. A **22**, L149 (1989).
[15] R. Monasson, Phys. Rev. Lett. **75**, 2847 (1995).
[16] S. Franz and G. Parisi, J. Phys. I (France) **5**, 1401 (1995).
[17] A. Barrat, S. Franz, and G. Parisi, J. Phys. A **30**, 5593 (1997).
[18] L. Zdeborová and F. Krzakala, Phys. Rev. B **81**, 224205 (2010).
[19] F. Krzakala and L. Zdeborová, J. Phys. Conf. Ser. **473**, 012022 (2013).
[20] G. Parisi and F. Zamponi, Rev. Mod. Phys. **82**, 789 (2010).
[21] P. Charbonneau, J. Kurchan, G. Parisi, P. Urbani, and F. Zamponi, Nat. Commun. **5**, 3725 (2014).
[22] M. Mezard and G. Parisi, in *Structural Glasses and Supercooled Liquids: Theory, Experiment, and Applications*, edited by P. G. Wolynes and V. Lubchenko (Wiley & Sons, New York, 2012).
[23] See Supplemental Material at http://link.aps.org/supplemental/10.1103/PhysRevLett.114.015701, which includes Refs. [24–35], for details of the derivation of the Franz-Parisi potential, and all the technical details needed to extract the physical results from it.
[24] J. Kurchan, G. Parisi, and F. Zamponi, J. Stat. Mech. (2012) P10012.
[25] J. Kurchan, G. Parisi, P. Urbani, and F. Zamponi, J. Phys. Chem. B **117**, 12979 (2013).
[26] P. Charbonneau, J. Kurchan, G. Parisi, P. Urbani, and F. Zamponi, J. Stat. Mech. (2014) P10009.
[27] M. Mézard and G. Parisi, J. Phys. Condens. Matter **12**, 6655 (2000).
[28] M. Mézard and G. Parisi, J. Chem. Phys. **111**, 1076 (1999).
[29] B. D. Lubachevsky and F. H. Stillinger, J. Stat. Phys. **60**, 561 (1990).
[30] H. Yoshino and M. Mézard, Phys. Rev. Lett. **105**, 015504 (2010).
[31] H. Yoshino, J. Chem. Phys. **136**, 214108 (2012).
[32] T. Rizzo, Phys. Rev. E **88**, 032135 (2013).
[33] M. Mézard, G. Parisi, and M. A. Virasoro, *Spin Glass Theory and Beyond* (World Scientific, Singapore, 1987).
[34] J.-P. Hansen and I. R. McDonald, *Theory of Simple Liquids* (Academic Press, London, 1986).
[35] F. Krzakala, A. Montanari, F. Ricci-Tersenghi, G. Semerjian, and L. Zdeborova, Proc. Natl. Acad. Sci. U.S.A. **104**, 10318 (2007).
[36] A short transient when $\tau_\alpha(T) \sim T_g$ exist, where the system is neither at equilibrium nor confined in a glass. However, because $\tau_\alpha(T)$ increases quickly around T_g, for slow coolings this temperature regime is extremely small and negligible.
[37] S. Franz, G. Parisi, and F. Ricci-Tersenghi (to be published).
[38] P. Charbonneau, A. Ikeda, G. Parisi, and F. Zamponi, Phys. Rev. Lett. **107**, 185702 (2011).
[39] E. Gardner, Nucl. Phys. **B257**, 747 (1985).
[40] M. Mariani, G. Parisi, and C. Rainone, arXiv:1411.0938 [Proc. Natl. Acad. Sci. U.S.A. (to be published)].
[41] B. P. Tighe, Granular Matter **16**, 203 (2014).
[42] H. Yoshino and F. Zamponi, Phys. Rev. E **90**, 022302 (2014).
[43] J. Ren, J. A. Dijksman, and R. P. Behringer, Phys. Rev. Lett. **110**, 018302 (2013).
[44] C. Coulais, A. Seguin, and O. Dauchot, Phys. Rev. Lett. **113**, 198001 (2014).
[45] M. Otsuki and H. Hayakawa, Phys. Rev. E **90**, 042202 (2014).
[46] L. Berthier, H. Jacquin, and F. Zamponi, Phys. Rev. E **84**, 051103 (2011).